Imaging Single Photons in Non-Separable States of Polarization and Spatial-Mode

Xinru Cheng and Enrique J. Galvez

Department of Physics and Astronomy, Colgate University, Hamilton, NY 13346, U.S.A.

ABSTRACT

Non-separable superpositions of polarization and spatial mode of a single photon produce a state that has a polarization that depends on the transverse position, and contains all states of polarization represented on the Poincaré sphere. We have done measurements of the space-dependent state of polarization of single photons prepared in distinct 2×2 (qubit-qubit) and 2×3 (qubit-qutrit) non-separable superpositions of Laguerre-Gauss spatial and polarization states. Detection was done by polarimetry of the light projected at distinct locations in the transverse plane. The polarization patterns had a C-point polarization singularity (lemon, star or monstar) at the center of the transverse wavefunction.

Keywords: Single photons, Entanglement, Polarization singularities, C-points

1. INTRODUCTION

The quantum nature of physical systems is one of the long-standing mysteries in physical science. The quantum of light, the photon, presents unique opportunities to understand and reconcile our limited understanding of quanta. It is now well accepted that light is made of photons and that a beam of light is a conglomerate of photons of similar if not identical properties. When we detect a 1 mW beam from a laser pointer, we collect 2.5×10^{15} photons per second. Yet these photons are not small sections of the beam. Rather, each photon occupies a light mode, which extends as far as the spatial mode in the transverse direction and as far as the coherence length in the longitudinal direction. A pure spatial mode is independent of the polarization, the pattern of oscillation of the electromagnetic field. In a traditional view, we are accustomed to picturing a photon of a quantum of light in a single Gaussian mode and in a given state of polarization.

It has been shown that photons can be in any type of spatial mode, including helical modes.[1–4] Non-separable superpositions, the fundamental structure of entanglement, presents intriguing possibilities, creating quantum states that have a space-variant polarization,[5,6] which are known classically as vector beams.[7] As we show here, a photon in a nonseparable superposition of spatial and polarization states yields a hybrid mode that does not carry a unique state of polarization in the transverse-position basis. It constitutes a different view of the quantum of light, which is predicted by quantum mechanics, but which also shows an aspect of the complexity of a single quantum of light not seen before.

Light has a well established and sound description in the classical domain, expressed in terms of electromagnetic waves that consist of electric and magnetic vector fields that oscillate and contort as the light propagates and interact with media. This view extends to the quantum domain, where the oscillations of the electromagnetic field are expressed in terms of a two-state quantum system. This two-dimensional space is conveniently represented by points on the surface of the Poincaré sphere. The latter represents circular states with points on the poles of the sphere, linear states with points along the equator, and elliptical states elsewhere. This representation is also convenient because states that are antipodes on the sphere are orthogonal to each other. Transformations of the state of polarization leading to geodesic paths on the sphere also add a type of geometric phase to the quantum wave function, known as the Pancharatnam-Berry phase.[8]

Non-separable superpositions of light modes in the classical description result in polarization singularity C-points. These are points or lines where the orientation of the polarization ellipses is singular. Scalar modes of

---

light contain phase singularities, or optical vortices, but these are solutions of the scalar wave equation, and so are common to separable states of light. In contrast, C-points are specific consequences of a non-separable superposition of polarization and spatial modes.

In this article we present a direct measurement of the light mode that is a result of a nonseparable superposition of polarization and spatial mode. In Sec. 2 we present the theoretical description. It is followed by Sec. 3 on the experimental procedure. We present the experimental results in Sec. 4, followed by discussion and conclusions.

2. THEORETICAL FRAMEWORK

Laguerre-Gauss (LG) modes are a complete set of paraxial modes.[9] In contrast to polarization, spatial modes form an infinite space. Thus, more information can be stored in spatial modes (such as an image) than in the polarization of a single photon.[10] LG modes are of interest because they carry orbital angular momentum. They carry a phase which varies as $\exp i\ell\phi$, where ϕ is the angular coordinate in a plane that is transverse to the propagation direction, and ℓ is an integer known as the topological charge. Thus, the wavefront of the light in an LG mode consists of ℓ-intertwined helices, and photons can exist in such spatial modes,[1] as demonstrated previously by our group.[3] The process for producing photon pairs, spontaneous parametric down conversion, conserves orbital angular momentum.[1, 11] We exploit this in our laboratory methods, as described below.

The traditional picture of a photon has it in a separable state of polarization and spatial mode. For example, one such mode can be

$$|\psi\rangle = |\ell\rangle|E\rangle, \tag{1}$$

where $|\ell\rangle$ represents an LG spatial mode with topological charge ℓ, and $|E\rangle$ represents a state of polarization. For example, the state $|0\rangle|H\rangle$ represents a photon with $\ell = 0$ and linearly polarized along the horizontal direction, just how we would picture the photons coming out of a laser. The classical picture for photons in this state is that of a paraxial Gaussian wave with planar of spherical wavefronts, with the electromagnetic field at every point being horizontally polarized. A more interesting state is

$$|\psi'\rangle = \frac{1}{\sqrt{2}} \left(|1\rangle|R\rangle + e^{i\delta}|0\rangle|L\rangle \right). \tag{2}$$

It is a superposition of a spatial mode with $\ell = 1$ right circularly polarized with a spatial mode with $\ell = 0$ left circularly polarized, and with a relative phase of δ. Such a state is straight forward to produce say with an interferometer, and to visualize it classically as a coherent superposition. However, as seen from the quantal point of view, it involves the state of a single photon that is nonseparable, which would measure a violation of Bell inequalities refuting realism but not nonlocality. There is debate whether this state can be called entangled or not because it involves a single photon.

From the previous discussion, a single photon in the state of Eq. 2 has a peculiar form: it contains (all) states of polarization correlated with the spatial coordinates. If points in the transverse plane are expressed in terms of polar coordinates (r, ϕ), we can decompose the spatial modes into continuous-variable states

$$|\ell\rangle = \int\int dr\, d\phi\, A_\ell r^{|\ell|+1} G(r) e^{i\ell\phi} |r, \phi\rangle, \tag{3}$$

where

$$A_\ell = \left(\frac{2^{|\ell|+1}}{\pi|\ell|!} \right)^{1/2} \frac{1}{w^{|\ell|+1}}; \tag{4}$$

is a normalization constant and $G(r) = \exp(-r^2/w^2)$ is a Gaussian function, with w representing the paraxial spatial width of the photon. We will assume planar wavefronts for simplicity. Replacing Eq. 3 into Eq. 2 yields

$$|\psi'\rangle = \frac{\sqrt{2}}{\sqrt{\pi}w} \int\int dr\, d\phi\, g(r) \left(\frac{\sqrt{2}}{w} r e^{i\phi}|R\rangle + e^{i\delta}|L\rangle \right) |r, \phi\rangle. \tag{5}$$

Because an arbitrary state of polarization can be expressed as a superposition of orthogonal states of polarization with distinct amplitudes and phases, a measurement of the photon in a particular location will find it in a unique state of polarization. For example, at $r = 0$ it is left circularly polarized, and at $r = r_l = w/\sqrt{2}$ it is linearly polarized along an axis oriented by $\theta = \phi/2 - \delta$ with respect to the horizontal. A theoretical modeling of the pattern, corresponding to the measured data is shown in Fig. 1(a) for $\delta = \pi/2$. Such polarization multiplicity of a single photon is quite intriguing, and distinct from a simplistic view of a photon. (i.e., in state $|\psi\rangle$). For $r < r_l$ ($r > r_l$) the states of polarizations are right-handed (left-handed) ellipses, with ellipticity given by

$$\epsilon = \tan\left[\frac{\pi}{4} - \tan^{-1}\left(\frac{w}{\sqrt{2}r}\right)\right]. \tag{6}$$

In the experiments we obtain the ellipse orientation and ellipticity via the measured normalized Stokes parameters s_1, s_2 and s_3: $\theta = \tan^{-1}(s_2/s_1)$ and $\epsilon = \cos^{-1} s_3$.
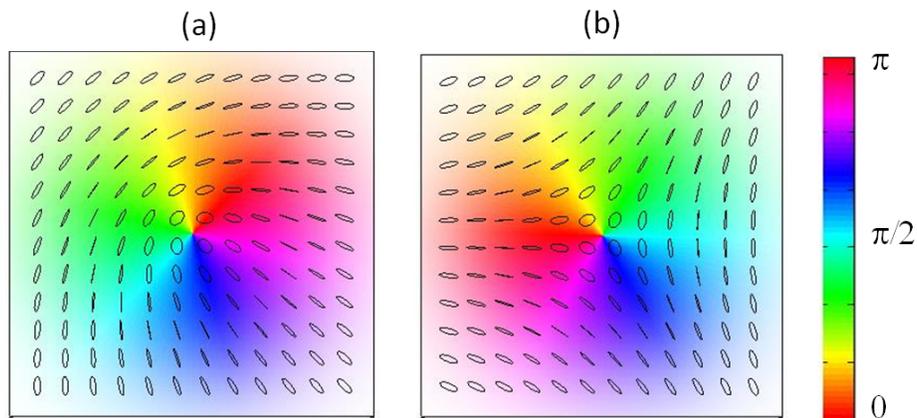
(a)   (b)

Figure 1. Theoretical modeling of the spatial projections of the polarization state of the light for: (a) the case of state $|\psi'\rangle$ (Eq. 2), which corresponds to a lemon polarization singularity pattern; and (b) the case of state $|\psi''\rangle$ (Eq. 7), which corresponds to a star polarization singularity pattern. Color denotes the orientation of the ellipses and color saturation corresponds to probability. $delta = \pi/2$ for both cases.

We can produce such a state classically with a coherent beam via superposition in an interferometer, where one beam has $\ell = 1$ and is right circularly polarized, and the other one is $\ell = 0$ and is left circularly polarized. The resulting beam is part of a class of beams called Poincaré beams.[12, 13] The interesting aspect of the state of Eq. 2 is that the transverse plane can be viewed as a mapping of the Poincaré sphere onto it.[13] Moreover, the polarization patterns in these beams are of intrinsic interest because they contain C-point singularities at points in the transverse plane where the component beams contain optical vortices. These points are singular in ellipse orientation, and so are circularly polarized.[13]

The state of Eqs. 2 and 5 produces a type of symmetric polarization singularity known as a left-handed lemon (Fig. 1(a)), where ellipse orientations rotate with the angular coordinate (at half the rate: $d\theta/d\phi = +1/2$). It is left-handed because the C-point and surrounding ellipses are left-handed. If we exchange the states of polarization, as in

$$|\psi''\rangle = \frac{1}{\sqrt{2}}\left(|1\rangle|L\rangle + e^{i\delta}|0\rangle|R\rangle\right), \tag{7}$$

we create a right-handed symmetric star, shown in Fig. 1(b), in which the surrounded ellipses rotate with the rate $d\theta/d\phi = -1$. Conversely, if instead of exchanging the states of polarization we use the spatial state $|-1\rangle$ with right-handed polarization, we would get a left-handed star.

The previous state is in a 4-dimensional space: formed by a spatial qubit and a polarization qubit. We can add a third spatial mode to form a spatial qutrit. A simple case, but of classical relevance is the one described by the state

$$|\psi'''\rangle = \frac{1}{\sqrt{2}} \left[(\cos\beta \,|+1\rangle + \sin\beta \, e^{i\gamma}|-1\rangle)|R\rangle + e^{i\delta}|0\rangle|L\rangle \right], \tag{8}$$

where β controls a superposition of two spatial eigenstates of unit topological charge but opposite sign, and γ the phase in between them.

The spatial state associated with right-handed polarization contains an asymmetric optical vortex. State $|\psi'''\rangle$ represents the full array of polarization singularities.[15] Except for the cases $\beta = 0, \pi/4, \pi/2$, they contain asymmetric singularities including a third type of C-point known as a monstar. The exact range of values of β that create a monstar depends on γ. For example, the least asymmetric cases arise for $\gamma = \pi$, leading to lemons for $0 > \beta > \beta_m$, with $\beta_m = \tan^{-1}(1/3) \simeq 18.43°$, monstars for $\beta_m < \beta < pi/4$ and stars for $\pi/4 < \beta < \pi/2$.

3. APPARATUS

The apparatus is shown in Fig. 2. We used a heralded photon source via spontaneous parametric down-conversion with type-I phase matching. Photons from a pump laser had a wavelength of 351 nm (argon-ion, 40-80 mW). We selected the degenerate non-collinear pairs with a wavelength of about 702 nm. The pump laser was focused to a waist of about 50 μm at the down-conversion crystal (beta-barium borate). The heralding photon was sent to a single-mode fiber (SMF), which projected the spatial mode of the photon to the $\ell = 0$ state. Because of orbital-angular-momentum correlations present in down-conversion, this projected the spatial mode of both down-converted photons.[10]

To encode the state of Eqs. 2 or 8, we used a 512×512 spatial light modulator (SLM), from Boulder Nonlinear Inc., in the reflection, as opposed to diffraction, mode. In this mode, the SLM encoded a phase pattern on the vertical component of the light, and just reflected the horizontal component. The half-wave plate (HWP) before the SLM was adjusted such that after loss due to pixelation diffraction in the SLM, there were two equal-amplitude polarization components after the SLM. An additional phase shifter before the SLM pre-compensated a phase introduced by a folding mirror after the SLM. This way, it controlled δ in Eq. 2. A quarter-wave plate immediately after the folding mirror converted linear polarization to circular polarization. This way, one polarization component was encoded with a spatial mode, and the other orthogonal component stayed with the incoming $\ell = 0$ spatial mode.

The type of state has been produced classically using a Mach-Zehnder type interferometer.[15] That arrangement works well with the (long) coherence lengths of coherent laser sources. However, the tight restrictions of large bandwith sources, as is the case of down-converted photons, adds challenges to the alignment and to decohering effects. One step in eliminating the decohering effect is to use a Sagnac type of interferometer, as done successfully before.[4] The present scheme is a new one, involving in-beam interference. Should we want to encode a mode also in the other polarization component, we would only need to rotate the polarization and send the light through a second SLM, where now the component with the spatial mode is just reflected, and the component in the Gaussian mode becomes encoded.

An example of the encoding of the general spatial mode of Eq. 8 is shown in the insert to Fig. 2. The superposition of two topological charges of different amplitudes yielded the phase structure of an optical vortex with a nonlinear phase gradient and with the same sign as the component of largest amplitude (controlled by β).

The next stage in the apparatus involved measuring the quantum state. This involved projecting the state into the position and polarization bases. Because the order of the projections does not change the result, we projected the polarization before we projected the position. For projecting the position we had a large-area (20 mm diameter) fiber collimator connected to a multimode fiber. This effectively acted as a bucket detector. Before it we had an adjustable iris that was scanned in a two dimensional plane via stepper motors, forming an $N \times N$ picture of the transverse intensity, with N set to a value between 10 and 20. Before the scanning iris was a polarization filter set to one of six polarization states: linear horizontal (H), linear vertical (V), linear diagonal (D), linear anti-diagonal (A), circular right (R) and circular left (L). These projections constituted a tomography

of the polarization qubit, yielding the Stokes parameters and a complete measurement of the polarization state: $S_0 = N_H + N_V$, $s_1 = (N_H - N_V)/S_0$, $s_2 = (N_D - N_A)/S_0$ and $s_3 = (N_R - N_L)/S_0$, where the last three are the normalized Stokes parameters, with N_i representing photon counts for filter i. Typically, maximum counts on a given scan were of the order of few hundred photon counts per second. We selected the polarization filter states using either the quarter-half-polarizer (QHP) or half-quarter-half-polarizer (HQHP) polarization filters, as shown in Fig. 2. The advantage of the 4-element filter is that the orientation θ and ellipticity ϵ of the state of polarization were controlled independently by the first and second half-wave plates, respectively.[13] This made it easier for calibrating the apparatus.
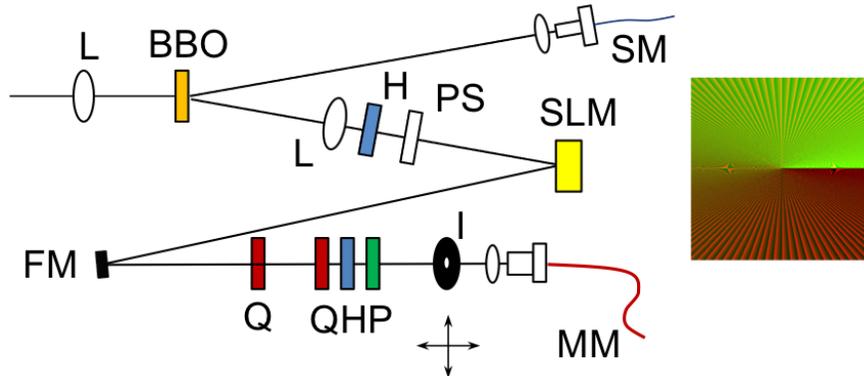

Figure 2. A schematic of the apparatus used to generate and encode non-separable states. It consists of lenses (L), a nonlinear crystal (BBO), single- and multi-mode fibers (SMF, MMF), quarter-wave plates (Q), half-wave plates (H), polarizers (P), phase-shifter (PS), folding mirror (FM) and a spatial light modulator (SLM). An x-y stage holding an iris (I) was moved by two motors in the transverse plane. The insert is an example of a bitmap we display on the SLM to encode a spatial mode onto the beam.
.

The photons collected by the fibers (single-mode for the heralding photon and multi-mode for the heralded photon) were passed through 40-nm band-pass filters centered at 702 nm, and were detected with avalanche photodiodes. An automated computer program acquired data, moving the stepper motors and recording the photon counts for specified time intervals. Six images were recorded for each setting of the polarization filter, and these were used to calculate the state of polarization of each projected point.

An example of the parameters for a given measurement, a scan with $N = 18$ had an iris diameter set to $d = 2$ mm. When the polarization filter was set to transmit the $|H\rangle$ state, the pixel with the highest intensity had about 340 single-photon counts (coincidences) per second. We took a full iris scan for each of the six settings of the polarization filter. The results shown in the next section correspond to point-by-point images taken under similar settings.

To verify that the light exhibited non-classical features we measured the degree of second order coherence $g_2(0)$ for a few conditions. This involved adding a beam splitter before the translating iris (left wide open), and a second wide collimator to capture all the light reflected by the beam splitter. This modification is not shown in the Fig. 2. In these measurements we detected the singles at the detectors, double coincidences with the heralding spatial-mode-projection detections, and triple coincidences. We did not scan the iris. We left is wide open and recorded the entire photon signal. We did this for all filter settings. In all cases we obtained $g_2(0) < 1$ (e.g., 0.62 ± 0.08), consistent with non-classical light.

4. RESULTS

The C-point lemon and star that results from polarimetry of the qubit-qubit state is shown in Fig. 3 (a) and (b), respectively. The C-point star pattern is generated from the same qubit-qubit state by reversing the first quarter-wave plate (QWP) after the SLM in the apparatus. The state of the photon in Figs. 3 (a) and (b)

correspond to those of Eqs. 2 and 7, respectively, but with a relative phase between the two terms of $\pi/2$. The data is plotted in the same way as Fig. 1: color denotes the orientation of the polarization ellipses, and saturation denotes photon counts. In the case of the figure, maximum saturation corresponds to about 2200 photon counts. The ellipses drawn at each data point correspond to the polarization ellipse obtained by doing a polarization tomography of the photon projected in the transverse position basis.
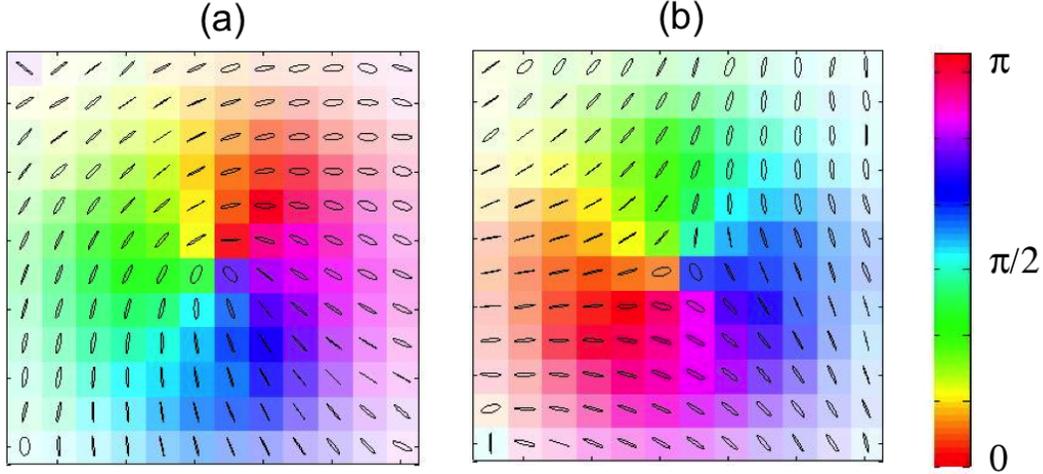

Figure 3. Images resulting from polarimetry of heralded single photons the qubit-qubit state, taken with pump laser power of 40 mW and with an iris diameter $d = 2$ mm. The scans were 12x12 pixels. The patternt of frames (a) and (b) correspond to a C-point lemon and star, respectively.

A comparison of the simulations of Figs. 1 with those of Fig. 3 show excellent agreement with no adjustable parameters. The experimental results are in remarkable agreement with previous measurements with classical light.[15] We also confirmed the rotation of the patterns with δ, which was varied by the phase shifter in Fig. 2.

We extended the previous analysis the qubit-qutrit state of Eq. 8, shown in Fig. 4. The spatial-mode basis is then composed of a superposition of topological charges $+1$ and -1 in a right-hand circular polarization state, with the spatial mode of topological charge 0 in a left-handed circularly polarized state. The superposition of the $+1$ and -1 modes is effected by the encoding in the SLM. The key element of this work is the projection of the spatial mode of the photon on its down-converted partner. This selects the spatial mode over a range that are produced by down-conversion, and reason that we can deliberately encode a spatial mode of our desire via the spatial mode. The component with the spatial mode with topological charge of zero is what remains by not altering its spatial mode.

The signature of a superposition of two optical vortices with $+1$ and -1 topological charges with *unequal* amplitudes is a mode with an optical vortex (that of the mode with greatest amplitude) but with a phase gradient that is not constant. The pattern programmed in the SLM, shown in the insert to Fig. 2, also shows this nonlinear phase variation. The nonlinearity then manifests in the symmetry of the pattern, as seen in Fig. 4. As the parameter β is varied, the variation of the change in the orientation of the polarization ellipses gets concentrated along the horizontal axis that passes through the center of the beam. The center of the pattern displays a polarization singularity C-point, with the one with $\beta = 0$ known as a lemon. As β increases one can see its effect on the polarization variation of the mode. The modes with $\beta = 20°$ and $\beta = 30°$ correspond to the monstar C-points. When $\beta = 45°$ there is no C-point, and the orientation changes abruptly from the top to the bottom of the pattern. Speaking in terms of spatial modes, the underlying spatial mode is a Hermite-Gauss one with a node along the horizontal axis. Past $\beta = 45°$ the underlying topological charge of the mode is -1, and the C-point pattern is a star. The one with $\beta = 60°$ has a nonlinear variation in the orientation, but the one with $\beta = 90°$ has a linear variation.

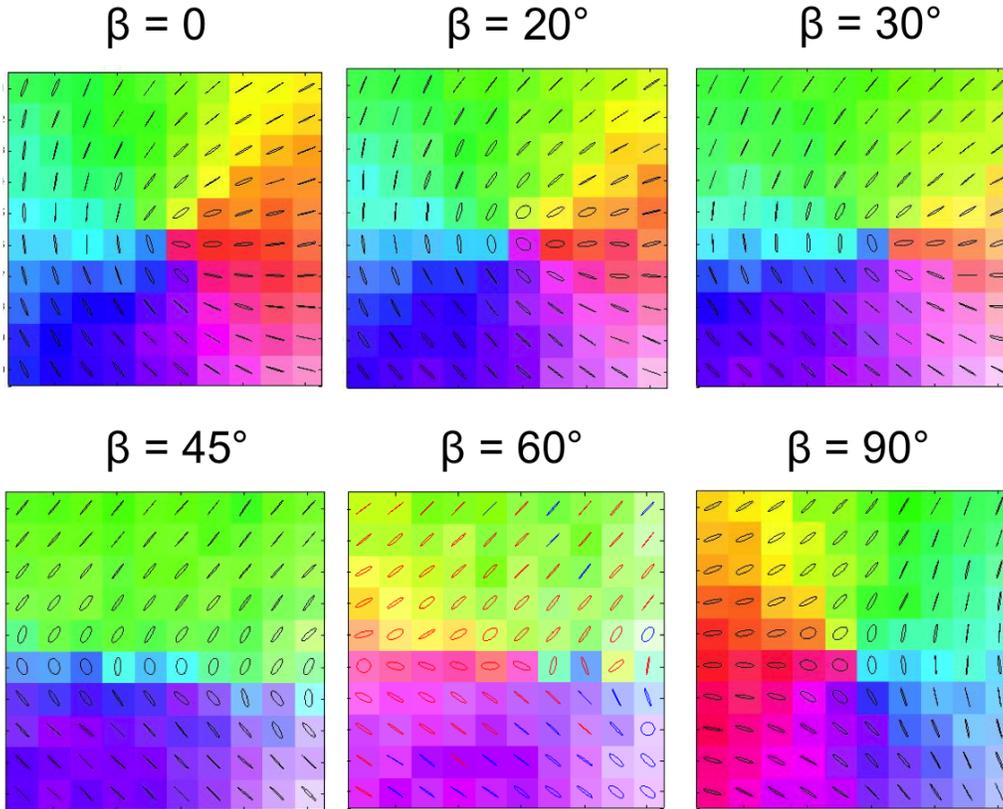**Figure 4.** Images resulting from polarimetry of the qubit-qubit state for different values of β.

An interesting question that we are currently investigating is the connection between the degree of polarization, defined by

$$\text{DoP} = \sqrt{s_1^2 + s_2^2 + s_3^2} \tag{9}$$

and the purity of the quantum state, defined by tomography tests, such as concurrence and linear entropy. Our preliminary analysis finds a degree of polarization that varies from point to point, being close to unity around the center, but reducing to about 0.4 in the center of the pattern. We are also in the process to set up and perform quantum state tomography of the states that we prepared. This question raises interesting prospects for using polarimetry of the spatially projected state to infer the purity of the quantum state. Recent work that prepare similar superpositions but with polarization entanglement with the partner photon shows a point by point variability in the entanglement.[14]

In summary, we have performed an experiment that prepares single photons in a non-separable state that exhibits C-point polarization singularities. Our data is in remarkable agreement with previous experiments done by our group with classical light.[15] The experiment is part of a program to produce entangled states of photons with desired states of polarization.[16] Toward this end, we have developed a way to encode the spatial modes onto single photons using same-path interferometry in connection with spatial light modulators. The experiments raise interesting prospects for understanding at a deeper level the connections between classical coherence and quantum information.[17, 18]

5. ACKNOWLEDGMENTS

REFERENCES

1. Mair, A., Vaziri, A.,Weihs, G., and Zeilinger, A., "Entanglement of the orbital angular momentum states of photons," Nature (London) **412**, 313-316 (2001).

2. Monken, C.H., Souto Ribeiro, P.H., and Padua, S., "Transfer of angular spectrum and image formation in spontaneous parametricdown-conversion," Phys. Rev. A **57**, 3123-3126 (1998).

3. Galvez, E. J., Coyle, L. E., Johnson, E., and Reschovsky, B. J., "Interferometric measurement of the helical mode of a single photon," New J. Phy. **13**, 053017 1-7 (2011).

4. Fickler, R. Lapkiewicz, R., Plick, W.N., Krenn, M., Schaeff, C., Ramelow, S., and Zeilinger, A., "Quantum entanglement of high angular momenta," Science **338**, 640-643 (2012).

5. Barreiro, J. T., Wei, T.-C., and Kwiat, P. G., "Remote preparation of single-photon hybrid entangled and vector-polarization states," Phys. Rev. Let. **105**, 030407 1-4 (2005).

6. Nagali, E., Sciarrino, F., De Martini, F., Marrucci, L., Piccirillo, B., Karimi, E., and Santamato, E., "Quantum information transfer from spin to orbital angular momentum of photons," Phys. Rev. Lett. **103**, 013601 1-4 (2009).

7. Zhan, Q., "Cylindrical vector beams: from mathematical concepts to applications," Adv. Opt. Photon. **1**, 1-57 (2009).

8. Kwiat, P.G., and Chiao, R.Y., "Observation of a nonclassical Berry's phase for a photon," Phys. Rev. Lett. **66**, 588-591 (1991).

9. Allen, L., Beijersbergen, M.W., Spreeuw, R.J.C., and Woerdman, J.P., "Orbital angular momentum of light and the transformation of Laguerre-Gaussian laser modes," Phys. Rev. A, **45**, 8185-8189 (1992).

10. Molina-Terriza, G., Torres, J.P., and Torner, L., "Twisted photons," Nature Phys. **3**, 305-310 (2007).

11. Torres, J.P., Alexandrescu, A., and Torner, L., "Quantum spiral bandwidth of entangled two-photon states," Phys. Rev. A **68**, 050301 (2003).

12. Beckley, A.M., Brown, T.G., and Alonso, M.A., "Full Poincaré beams," Opt. Express **18**, 10777-10785 (2010).

13. Galvez, E.J., Khadka, S., Schubert, W.H., and Nomoto, S. "Poincaré-beam patterns produced by nonseparable superpositions of LaguerreGauss and polarization modes of light," Appl. Opt. **51**, 2925-2934 (2012).

14. Fickler, R., Lapkiewicz, R., Ramelow, S., and Zeilinger, A., "Quantum entanglement of complex photon polarization patterns in vector beams," Phys. Rev. A **89**, 060301 1-5 (2014).

15. Galvez, E. J., Rojec, B. L., Kumar, V., and Viswanathan, N. K., "Generation of isolated asymmetric umbilicus in light's polarization," Phys. Rev. A **89**, 031801 (2014).

16. Galvez, E.J., "Proposal to produce two and four qubits with spatial modes of two photons," Proc. SPIE **8274**, 827415 (2012).

17. Kagalwala, H., Di Giuseppe, G., Abouraddy, A.F., and Saleh, B.E.A., "Bells measure in classical optical coherence," Nature Photonics **7**, 72-78 (2013).

18. De Zela, F., "Relationship between the degree of polarization, indistinguishability, and entanglement," Phys. Rev A **89**, 013845 (2014).